Eur Biophys J (1989) 17: 5–11

European Biophysics Journal

Solution structure of human plasma fibronectin as a function of NaCl concentration determined by small-angle X-ray scattering

B. Sjöberg[1]*, M. Eriksson[1], E. Österlund[2], S. Pap[1], and K. Österlund[2]

[1] Department of Medical Biochemistry, University of Göteborg, Box 33031, S-400 33 Göteborg, Sweden
[2] Department of Biochemistry, University of Helsinki, Unioninkatu 35, SF-00170 Helsinki 17, Finland

Received June 13, 1988 / Accepted in revised form November 14, 1988

Abstract. The structure of human plasma fibronectin in 50 m*M* *Tris*-HCl buffer, pH 7.4, containing varying concentrations of NaCl, has been investigated using the small-angle X-ray method.

Below 0.3 *M* NaCl the overall structure of the molecule is disc-shaped; at 0 *M* NaCl the axial ratio of the disc is about 1:7 and between 0.1 *M* to 0.3 *M* it is slightly more asymmetric, with an axial ratio of 1:10.

At about 0.3 *M* NaCl there is a reversible transition to a more open structure, and, from 0.3 *M* up to 1.1 *M* NaCl the small-angle X-ray data can be explained by models consisting of ensembles of flexible, non-overlapping, bead-chains generated by a Monte Carlo procedure. Within this concentration range there is a gradual increase in the stiffness of the chains, as well as a decrease in bead radius, which indicates that the molecule becomes more open when the NaCl concentration is increased.

The transition to a more open structure is also demonstrated by the average radius of gyration which increases gradually from 8.26 nm at 0 *M* NaCl to 8.75 nm at physiological or near-physiological conditions, and up to 16.2 nm at 1.1 *M* NaCl.

Key words: Human plasma fibronectin, solution structure, ionic strength, flexible bead-chain models, Monte Carlo simulation, small-angle X-ray scattering

Introduction

Human plasma fibronectin (hpFN) is an adhesive glycoprotein of molecular weight about 520,000. It has affinity for many types of ligands, such as collagen, fibrin, fibrinogen, DNA and certain cell surfaces. This affinity is the basis for the functions attributed to hpFN, e.g. cell-cell and cell-substrate adhesion, cell spreading, embryogenesis, wound healing, nerve regeneration and phagocytosis (for reviews, see Yamada 1983; McDonagh 1985; Akiyama and Yamada 1986).

The molecule consists of two, nearly identical, subunits connected covalently close to their carboxy termini by disulfide bonds. It is a rather unique protein in the sense that it is made up of structural, and functional, domains; the primary structure mostly consists of three different types of repeats (homologies I, II and III), varying in size from about 40 to 90 amino acids (Kornblihtt et al. 1985; Skorstengaard et al. 1986), and each of the structural domains contains one or more of the repeats. Such a structure opens the possibility for a molecule with very flexible properties, and hpFN is probably one of the most versatile proteins investigated so far. For instance, the structure of hpFN has been found to depend very much on solution conditions. The knowledge of the structural behaviour of this multifunctional molecule would greatly help to understand its reactions and biological functions.

In solution at physiological, or near-physiological, conditions hpFN maintains a compact, but still rather asymmetric, shape. By using the small-angle X-ray and neutron scattering techniques it was found that the overall shape of the molecule can be approximated as a disc with an axial ratio of 1:10 (Sjöberg et al. 1987). A result which can also fully explain the rather extreme hydrodynamic properties reported for hpFN, under these conditions.

The compact form is transformed to a more open structure upon increasing the ionic strength and/or when changing the pH, indicating that electrostatic interactions play a major role in the folding of the molecule. Data obtained by several different experimental methods indicate that the molecule retains its major regions of tertiary structure upon transition to the more open structure (McDonagh 1985; Lai et al. 1984).

* To whom offprint request should be sent

Abbreviations: hpFN, human plasma fibronectin; SAXS, small-angle X-ray scattering; *Tris*, *tris* (hydroxymethyl) aminomethane; DTT, dithiothreitol; BA, benzamidine hydrochloride; PMSF, phenylmethylsulfonyl fluoride

Electron micrographs of hpFN have shown the molecule both as a compact, globular particle (Koteliansky et al. 1981) and as a slender strand (Engel et al. 1981; Odermatt et al. 1982; Erickson and Carrell 1983). It has been shown that the results obtained by electron microscopy depend on the technique used for preparing the samples (Price et al. 1982). The electron micrographs of the slender strand, however, show some interesting features: there is a bend in the middle forming an average angle of 70°, and the molecule is flexible; it can indeed be visualised as a flexible string of beads. In fact, flexible bead-chain models, of varying stiffness, have been used successfully by Rocco et al. to explain both the hydrodynamic properties (1983) and the radius of gyration determined by light scattering (1987).

The solution structure of hpFN has already been investigated under physiological conditions using the small-angle X-ray and neutron scattering techniques (Sjöberg et al. 1987). In this work we use the small-angle X-ray technique to follow the change in structure of the hpFN molecule upon increasing the NaCl concentration from 0 to 1.1 *M*. The main results indicate that the disc shaped particle exists up to about 0.3 *M* NaCl. Above this concentration the data can be explained by ensembles of flexible bead-chain models generated by a Monte Carlo procedure; at increasing NaCl concentration there is a gradual increase in the stiffness of the chain, as well as a decrease in the bead radius. There is also a small structural change of hpFN which occurs at very low NaCl concentrations; at 0 *M* NaCl the axial ratio is about 1:7, whereas after addition of NaCl it increases to about 1:10.

Materials and methods

Preparation of the hpFN-samples

hpFN was purified using a modification of the method described by Vuento and Vaheri (1979). Fresh blood was taken from healthy volunteers directly to 3.8% (w/v) sodium citrate containing 25 m*M* BA and 5 m*M* PMSF (four parts blood and one part citrate solution). All buffers used for the chromatography on Sepharose and gelatin-Sepharose also contained 5 m*M* BA and 1 m*M* PMSF to inhibit possible protease activity. hpFN was eluted from the arginine-Sepharose column by a buffer containing 0.5 *M* NaCl, 0.02% NaN_3, 50 m*M* *Tris*-HCl pH 7.5. The purified hpFN showed a single line on immunoelectrophoresis, and Ouchterlony double immunodiffusion, when developed against anti-whole human serum and anti-hpFN prepared in rabbits. On sodium dodecylsulfate polyacrylamide gel electrophoresis a single band was seen in the position expected for intact hpFN and, after reduction of disulfide bonds using DTT, a closely spaced doublet was seen in the position expected for the subunits. No lower molecular weight bands was seen even when developed with a sensitive silver stain (Bio-Rad Laboratories, Richmond, CA).

Before the SAXS-measurements hpFN was dialysed against a buffer containing 50 m*M* *Tris*-HCl, pH 7.4. Protein concentration was determined spectrophotometrically at 280 nm using $A^{1\%}_{1\,cm} = 12.8$ (Mosesson et al. 1975). Samples containing NaCl were prepared by mixing the dialysed protein solution with either solid NaCl, or with a stock solution of high NaCl concentration. Background solutions were prepared by using the same procedure, except that dialysis buffer was used instead of the protein solution. Electron densities of the solvents, at the different NaCl concentrations used, were calculated from the solution densities determined using a digital densitometer (Kratky et al. 1969). The main part of the scattering data were recorded for protein concentrations in the range from 4 to 10 mg/cm^3.

Small-angle X-ray scattering measurements

The SAXS-data were recorded with the monitor type of small-angle X-ray camera developed by Kratky et al. (1971) which was set up in a room thermostatted at 21.0 °C. The sample container was an ordinary thin-walled Debye-Sherrer glass capillary. Monochromatization of the copper radiation from a sealed-tube X-ray source was made with a nickel filter and a pulse-height selector, together with a proportional counter. Absolute intensities for the molecular weight calculations were obtained using a calibrated Lupolen sample (Kratky et al. 1966). Intensity data were recorded with an on-line Commodore PC10 computer.

Methods of computation

Three different types of models have been used in this work. At low NaCl concentrations the data can be explained by ellipsoids of revolution; the scattering from such a particle is easily calculated (Guinier and Fournet 1955). At higher NaCl concentrations we obtained a fairly good fit by using the equation (Debye 1947)

$$I(Q) = (2/x^2) \cdot \{\exp(-x) + x - 1\};\ x = (R \cdot Q)^2, \qquad (1)$$

which assumes a flexible chain molecule. In Eq. (1) R is the radius of gyration and $Q = (4\pi/\lambda)\sin\xi$. The X-ray wavelength is denoted by λ and ξ is half the scattering angle. This indicates that the hpFN molecule, at higher NaCl concentrations, behaves like a flexible

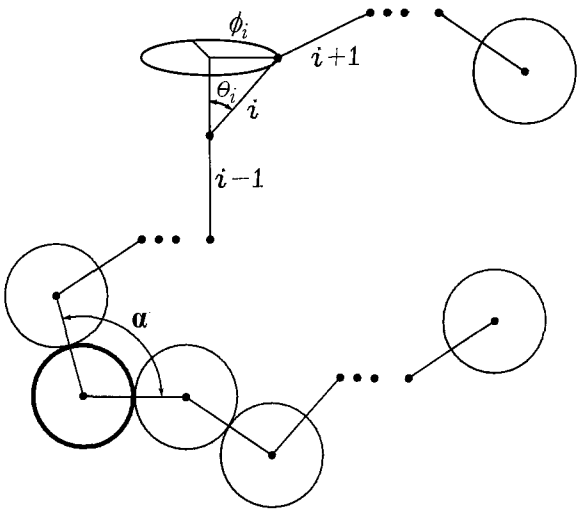

Fig. 1. Definition of the bead-chain model used in the Monte Carlo simulations. Successive, non-overlapping, beads are generated from a starting bead (drawn with the *heavy line*) in two directions forming an angle α. The longitudinal angles ϕ_i assume any value between 0 and 2π with equal probability. Stiffness of the chain is introduced by generating random latitudinal angles θ_i from a distribution which assumes an energy of bending quadratic in θ_i. All the total N beads per molecule are assumed to have the same radius r

chain molecule. The Debye equation, Eq. (1), however, fails to explain the whole scattering curve, especially at higher Q-values. A much better fit was obtained using a Monte Carlo approach where we try to simulate the behaviour of the hpFN molecule in more detail. This method will be described below.

The Monte Carlo approach

Here we calculate the average scattering curve which will be obtained from an ensemble of random bead-chains. The generation of each individual molecule starts with a central bead (drawn with a heavy line in Fig. 1). Next the two arms, of identical length, are generated by starting in two directions which form a kink angle α with each other. Randomness of consecutive beads is introduced by assuming that the longitudinal angles ϕ_i assume any value between 0 and 2π with equal probability (the random ϕ-model, Schellman 1974). The stiffness of the chain is considered by assuming an energy of bending quadratic in the latitudinal angles θ_i. This corresponds to a restoring force proportional to θ_i. Thus the probability distribution function takes the form (Schellman 1974)

$$P(\theta) = C \cdot \exp\{-\theta^2/(2\sigma^2)\} \cdot \sin\theta, \tag{2}$$

where C is a normalisation constant, the exponential function corresponds to the Bolzmann distribution function and $\sin\theta$ is the latitudinal weighting function. The parameter σ determines the stiffness of the chain; small σ corresponds to a stiff, extended, chain and large σ to a coiled chain.

Individual random chains were constructed by successive applications of the rotational matrix (Goldstein 1959)

$$A_i = \begin{bmatrix} \cos\theta_i & -\sin\theta_i & 0 \\ \sin\theta_i \cdot \cos\phi_i & \cos\theta_i \cdot \cos\phi_i & -\sin\phi_i \\ \sin\theta_i \cdot \sin\phi_i & \cos\theta_i \cdot \sin\phi_i & \cos\phi_i \end{bmatrix}. \tag{3}$$

Thus the coordinates of the ith bead are transformed to the coordinate frame of the bead number $i-1$ by multiplication with the matrix A_i. Uniformly distributed random values of ϕ_i between 0 and 2π were generated by using the subroutine G05CAF from the NAG-Fortran library (1983). Latitudinal angles θ_i were obtained by generating random numbers from the distribution function (2) by using the acceptance-rejection technique suggested by von Neumann (1951). That is, first $P(\theta)$ is scaled to be $\leq \theta_{\max}$, and then a pair of uniformly distributed random numbers θ_1 and θ_2 are generated from the interval $(0, \theta_{\max})$. If $\theta_2 \leq P(\theta_1)$ we accept θ_1 as a random number from the distribution (2), if that condition is not fullfilled, we reject the pair and generate a new pair of random numbers. The procedure was tested, and found to work well, by generating sets of 10^5 random numbers and comparing them with the true curve predicted by Eq. (2).

During the successive generation of the chains a check for overlapping beads was made; if overlapping occurred new random numbers were generated until chains completely free from overlapping were obtained.

After the coordinates of all the beads of one individual chain were generated, as described above, the corresponding scattering curve was calculated by using the formula (Debye 1915)

$$I(Q) = \Phi^2(r) \cdot \left\{ N + 2 \sum_{i=1}^{N-1} \sum_{j=i+1}^{N} \sin(Q \cdot d_{ij})/(Q \cdot d_{ij}) \right\}, \tag{4}$$

where $\Phi^2(r)$ is the scattering from a spherical bead of radius r; it was assumed that all the beads have the same radius; d_{ij} is the distance between beads i and j. The total number of beads per molecule, N, was obtained simply by dividing the total volume of the hpFN molecule with the bead volume. The whole process was repeated and, for the final calculations, one thousand individual scattering curves were averaged, in order to obtain the scattering for the total assembly of particles.

The number of individual scattering curves used in the averaging process was chosen as a compromise between accuracy and computer time. As a practical test, to see whether the number of individual chains was enough, we simply repeated the calculations and

checked for deviations in the final results. We found that the generation of one thousand chains was enough to obtain convergence to a unique result within the accuracy of our experimental data. This was also a check for systematic biases arising from nonrandomness in the pseudorandom numbers.

The parameters describing the system (α, σ, r, and N), were obtained directly from the slit-smeared intensity data by using a general non-linear least-squares method (Sjöberg 1978). In these calculations we found it most practical to keep the kink angle α fixed, equal to 70°, which is the angle seen on electron micrographs of hpFN. Also, the total number of beads per molecule N, was obtained by assuming the total volume of the hpFN molecule to be approximately equal 1,100 nm^3, which is the average volume obtained at low NaCl concentrations. Thus only the parameters σ and r were refined.

Results and discussion

From the results summarised in Table 1 it follows that the structural transition of the hpFN molecule from a compact to a more open structure occurs at about 0.3 M NaCl. Below that value the experimental small-angle X-ray data can be explained by ellipsoid-of-revolution-shaped compact bodies. Above 0.3 M NaCl we have to assume ensembles of bead-chains in order to be able to explain the data. Figure 2 shows the experimental X-ray intensity points together with theoretical curves calculated using the parameters given in Table 1.

In fact, there is also a small, but distinct, structural transition which occurs at very low NaCl concentrations; the molecule is slightly less asymmetric at 0 M as compared with 0.1 M NaCl. The semiaxes reported at 0 M NaCl are taken as averages of six different determinations and they are clearly different from the values given at higher NaCl concentrations. From 0.1 M up to 0.22 M NaCl the dimensions seem to be independent of the NaCl concentrations; the apparent variations in the semiaxes given in Table 1, for this NaCl region, cannot be considered as significant since they are within the accuracy of the method. The larger relative variations of the c-axis compared with the a- and b-axes are due to the fact that the short dimension is mainly determined by the outer part of the scattering curve where the errors are larger due to the smaller difference in scattering between the buffer and the protein solution.

Thus, below about 0.3 M NaCl the X-ray data are consistent with a condensed, but rather asymmetric, molecule. A result which can also explain the rather abnormal hydrodynamic parameters reported for hpFN (Sjöberg et al. 1987).

At 0.315 M NaCl we simply assumed the solution to contain a mixture of ellipsoids and bead-chains with the parameters given in Table 1, and we only refined their relative concentrations using the least-squares computer program (Sjöberg 1978). We obtained the result that 75% of the total population of hpFN molecules are present as ellipsoids, and the remaining 25% as bead-chains. As can be seen from Fig. 2 the experimental data can be well explained by this model. We cannot, however, judge from the present data, if that is the true situation or if the structural changes occur in very small steps so that the solution contains ellipsoids which are just starting to unfold.

Table 1. Summary of the results obtained by the least-squares refinement. At NaCl concentrations below, or equal to, 0.221 M the data can be explained by ellipsoids of revolution with semiaxes $a=b$ and c. Above 0.3 M NaCl we have to assume flexible bead-chain Monte Carlo models defined by the stiffness parameter σ and bead radius r. The kink angle α was kept constant at 70° and the number of beads per molecule N, was chosen to give a total volume equal to about 1,100 nm^3. At 0.315 M NaCl we obtained the result that 75% of the population of the hpFN molecules are present as ellipsoids, and the remaining 25% as bead-chains, with the parameters indicated. The average radii of gyration, $\sqrt{<R^2>}$, were calculated from the geometrical dimensions of the models

[NaCl] [M]	$a=b$ [nm]	c [nm]	σ [rad]	r [nm]	N	$\sqrt{<R^2>}$ [nm]
0	13.0	1.79	-	-	-	8.26
0.100[a]	13.8	1.44	-	-	-	8.75
0.152	13.9	1.27	-	-	-	8.81
0.199[b]	13.8	1.36	-	-	-	8.75
0.221	13.8	1.39	-	-	-	8.75
0.315	13.8	1.39	1.50	2.58	15	9.42
0.416	-	-	1.50	2.58	15	11.2
0.556	-	-	1.10	1.92	37	14.9
0.815	-	-	1.07	1.85	41	15.6
1.064	-	-	0.99	1.76	47	16.2

[a] from Sjöberg et al. (1987)
[b] not shown in Fig. 2

Fig. 2. Experimental, slit-smeared small-angle X-ray intensity points, $\tilde{I}$, after normalizing with protein concentration, compared with theoretical model curves calculated on the basis of the parameters given in Table 1. At 0 M NaCl intensity data are given for the following concentrations of hpFN: 7.5 mg/cm^3 (open circles) and 4.5 mg/cm^3 (crosses); at 1.064 M NaCl: 6.6 mg/cm^3 (open circles) and 9.7 mg/cm^3 (crosses). All other intensity data shown were recorded with protein concentrations within the range from 6 to 10 mg/cm^3. The intensities are drawn only on a relative scale, owing to the difference in contrast, and difference in scattering power, as a function of NaCl concentration

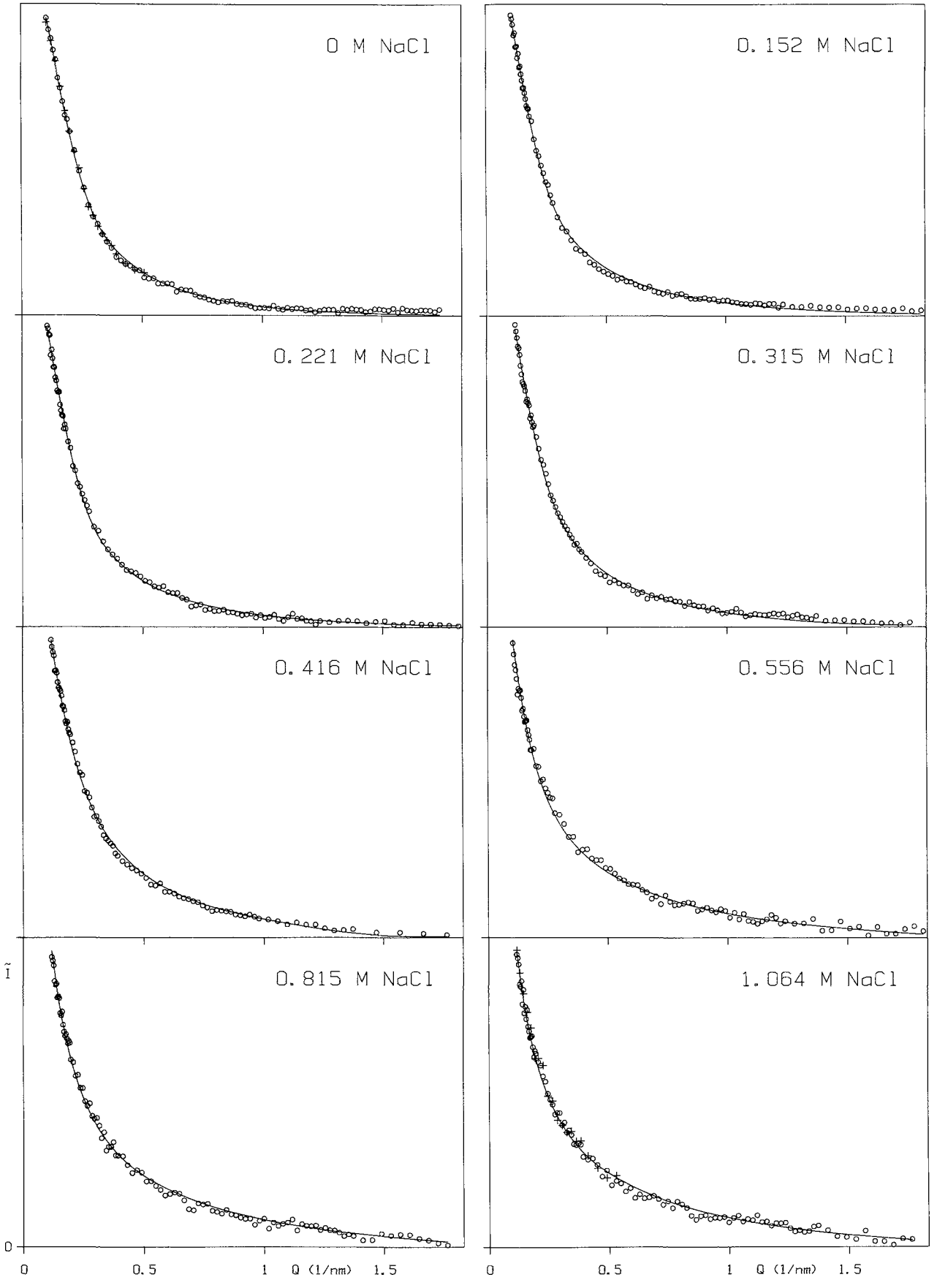
0 M NaCl
0.152 M NaCl
0.221 M NaCl
0.315 M NaCl
0.416 M NaCl
0.556 M NaCl
0.815 M NaCl
1.064 M NaCl
Ĩ
0
0
0.5
1
Q (1/nm)
1.5

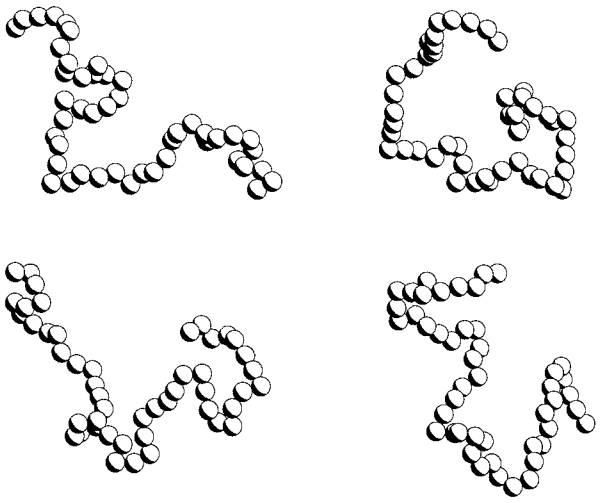

Fig. 3. Some typical examples of random bead-chains generated as described in the text for $\sigma = 0.99$ rad, $r = 1.76$ nm and $N = 47$. During the Monte Carlo simulation average small-angle X-ray scattering curves for ensembles of one thousand such random chains were calculated

Above 0.3 *M* NaCl we were unable to explain the data with simple three-axial bodies. Relatively good fits were obtained with Eq. (1), which assumes a flexible Gaussian coil. This indicates that the molecule is flexible, and has some similarity with a Gaussian coil. Much better fits were, however, obtained with the ensembles of bead-chains generated by the Monte Carlo procedure. This is also in agreement with the results obtained by Rocco et al. in their studies using hydrodynamic techniques (1983) and light scattering (1987), where similar types of bead-chains were used to explain the data.

It might be argued that the observed effect is an indication of aggregation of the hpFN molecule rather than a change in conformation. In order to check for aggregation we have calculated the molecular weight at each NaCl concentration using Eq. (1) in Sjöberg et al. (1987). The forward scattering, $I(0)$, was obtained from the least-squares program (Sjöberg 1978) and the scattering densities of the solvents, ϱ_S, were calculated from the densities of the solvents, at each NaCl concentration. For all the data, recorded at the different NaCl and hpFN concentrations, we obtained the average values $530{,}000 \pm 30{,}000$ which is in excellent agreement with previous determinations using X-ray and neutron-scattering (Sjöberg et al. 1987) and light scattering (Rocco et al. 1987); 510,000, 530,000 and 533,000, respectively.

In a previous investigation of hpFN at 0.10 *M* NaCl (Sjöberg et al. 1987) it was found that interparticle scattering effects are negligible within the concentration range up to 11 mg/cm^3. A check for interparticle scattering was performed also in this work by recording scattering data at several different protein concentrations. In Fig. 2 we show the result only for 0 *M* and 1.064 *M* NaCl. After normalizing for the concentration we obtain coinciding curves which means that interparticle scattering can be neglected. This is also a check for protein-concentration dependent aggregation of hpFN.

The bead-chain model is, of course, a mathematical simplification of the real situation. We also refine only the stiffness parameter σ and the bead radius r. The kink angle α is kept constant at 70°, which is the angle seen on the electron micrographs of hpFN. The number of beads N per molecule is obtained from the condition that the volume of the molecule is equal to about 1,100 nm^3 and the beads of our model should not be confused with the functional domains of the molecule.

The model does, however, explain the experimental SAXS-data (Fig. 2) and it also demonstrates some of the properties of the molecule. For instance, the increase in stiffness, with increasing NaCl concentration is shown by the decrease in σ (Table 1). From the decrease in bead radius r it follows that the structure gradually becomes more open and elongated when the NaCl concentration is increased. Examples of some typical bead-chains are shown in Fig. 3.

The structural transition from a condensed to a gradually more open structure is also demonstrated by the average radius of gyration (Table 1). This parameter increases from 8.26 nm at 0 *M* NaCl to 8.75 nm at physiological or near-physiological conditions, and up to 16.2 nm at 1.1 *M* NaCl. The values of the radii of gyration obtained by SAXS are slightly lower than the corresponding values obtained by light scattering, 10.7 nm at 0.16 *M* and 17.5 nm at 1.01 *M* ionic strength (Rocco et al. 1987).

The structural transition from a condensed to a more open structure has been found to be reversible when studied by hydrodynamic and spectroscopic techniques (Markovic et al. 1983). We have also tested for reversibility by dialysing a sample of hpFN exposed to 1 *M* NaCl against the 50 m*M* *Tris*-HCl buffer; also within the resolution of the small-angle X-ray technique the reaction was found to be fully reversible. Reversibility can, of course, also be expected from the fact that hpFN is exposed to 1 *M* NaCl during the preparation (Vuento and Vaheri 1979) although it might be argued that the protein is protected when it is bound to the gelatin-Sepharose column.

The continuous transition of hpFN from a condensed to an open structure, over a large NaCl range, is rather uncommon compared with many other (smaller) proteins (Creighton 1984). Usually such a transition is a cooperative process which occurs over a sharp range in the disturbing parameter, and there are only two molecular forms dominating. One expla-

nation for the odd behaviour of hpFN may be that it is composed of domains, and each domain acts relatively independent of other domains.

Acknowledgements. This work was supported by grants from the Swedish Natural Science Research Council.

References

Akiyama SK, Yamada KM (1986) Fibronectin. Adv Enzymol 59:1–57

Creighton TE (1984) Proteins, structures and molecular properties. WH Freeman, New York

Debye P (1915) Zerstreuung von Röntgenstrahlen. Ann Physik 46:809–823

Debye P (1947) Molecular-weight determination by light scattering. J Phys Colloid Chem 51:18–32

Engel J, Odermatt E, Engel A, Madri JA, Furthmayr H, Rohde H, Timpl R (1981) Shapes, domain organizations and flexibility of laminin and fibronectin, two multifunctional proteins of the extracellular matrix. J Mol Biol 150:97–120

Erickson HP, Carrell NA (1983) Fibronectin in extended and compact conformations. Electron microscopy and sedimentation analysis. J Biol Chem 258:14539–14544

Goldstein H (1959) Classical mechanics. Addison-Wesley, Reading, Massachusetts, USA

Guinier A, Fournet G (1955) Small-angle scattering of X-rays. John Wiley, New York

Kornblihtt AR, Umezawa K, Vibe-Pedersen K, Baralle FE (1985) Primary structure of human fibronectin: differential splicing may generate at least 10 polypeptides from a single gene. EMBO J 4:1755–1759

Koteliansky VE, Glukhova MA, Bejanian MV, Smirnov VN, Filimonov VV, Zalite OM, Venyaminov SY (1981) A study of the structure of fibronectin. Eur J Biochem 119:619–624

Kratky O, Pilz I, Schmitz PJ (1966) Absolute intensity measurement of small angle X-ray scattering by means of a standard sample. J Colloid Interface Sci 21:24–34

Kratky O, Leopold H, Stabinger H (1969) Dichtemessungen an Flüssigkeiten und Gasen auf 10^{-6} g/cm^3 bei 0.6 cm^3 Präparatvolumen. Z Angew Physik 27:273–277

Kratky O, Leopold H, Seidler H-P (1971) Röntgen-Kleinwinkelkamera mit Monitor. Z Angew Physik 31:49–50

Lai C-S, Tooney NM, Ankel EG (1984) Structure and flexibility of plasma fibronectin in solution: Electron spin resonance spin-label, circular dichroism, and sedimentation studies. Biochemistry 23:6393–6397

Markovic Z, Lustig A, Engel J, Richter H, Hörmann H (1983) Shape and stability of fibronectin in solutions of different pH and ionic strength. Hoppe-Seyler's Z Physiol Chem 364: 1795–1804

McDonagh J, Ed (1985) Plasma fibronectin, structure and function. Marcel Dekker, New York.

Mosesson MW, Chen AB, Huseby RM (1975) The cold-insoluble globulin of human plasma: Studies of its essential structural features. Biochim Biophys Acta 386:509–524

NAG-Fortran manual (1983) Numerical Algorithms Group Ltd, NAG Central office, Mayfield House, 256 Banbury Road, Oxford OX2 7DE, UK

von Neumann J (1951) Various techniques used in connection with random digits. Natl Bur Stand, Appl Math Series 12:36–38

Odermatt E, Engel J, Richter H, Hörmann H (1982) Shape, conformation and stability of fibronectin fragments determined by electron microscopy, circular dichroism and ultracentrifugation. J Mol Biol 159:109–123

Price TM, Rudee ML, Pierschbacher M, Ruoslahti E (1982) Structure of fibronectin and its fragments in electron microscopy. Eur J Biochem 129:359–363

Rocco M, Carson M, Hantgan R, McDonagh J, Hermans J (1983) Dependence of the shape of the plasma fibronectin molecule on solvent composition. Ionic strength and glycerol content. J Biol Chem 258:14545–14549

Rocco M, Infusini E, Daga MG, Gogioso L, Cuniberti C (1987) Models of fibronectin. EMBO J 6:2343–2349

Schellman JA (1974) Flexibility of DNA. Biopolymers 13:217–226

Sjöberg B (1978) A general, weighted least-squares method for the evaluation of small-angle X-ray data without desmearing. J Appl Crystallogr 11:73–79

Sjöberg B, Pap S, Österlund E, Österlund K, Vuento M, Kjems J (1987) Solution structure of human plasma fibronectin using small-angle X-ray and neutron scattering at physiological pH and ionic strength. Arch Biochem Biophys 255:347–353

Skorstengaard K, Jensen MS, Sahl P, Petersen TE, Magnusson S (1986) Complete primary structure of bovine plasma fibronectin. Eur J Biochem 161:441–453

Vuento M, Vaheri A (1979) Purification of fibronectin from human plasma by affinity chromatography under non-denaturing conditions. Biochem J 183:331–337

Yamada KM (1983) Cell surface interactions with extracellular materials. Annu Rev Biochem 52:761–799